Transition from Surface to Volume Expansion in Argon Clusters Coulomb Explosion

D. Komar,[1] K. Raspe,[1] L. Kazak,[1,2] N. Iwe,[1] K.-H. Meiwes-Broer,[1,3] and J. Tiggesbäumker[1,3,*]
[1]Institute of Physics, University of Rostock, 18059 Rostock, Germany
[2]Institute for Quantum Optics, Ulm University, 89081 Ulm, Germany
[3]Department "Life, Light and Matter", University of Rostock, 18059 Rostock, Germany

(Received 7 February 2024; accepted 25 June 2024; published 16 August 2024)

The intensity-difference spectrum technique is applied to record charge-state resolved ion energy spectra from the Coulomb explosion of small Ar clusters under well-resolved laser intensity conditions. The far-reaching control of the experimental parameters permits us to identify a striking change in the expansion pattern of the nanoplasma beyond a given intensity. The simultaneous characterization of ion charge state and energy uncovers that a reduction of the laser intensity leads to a development of low energy cuts in the ion yields, not present at higher fluence. The complex interplay of outer ionization, recombination, ion screening, and the phenomenon of ionization saturation favors a surface-driven expansion at low plasma electron temperatures. With increasing laser intensity a transition into a volume-driven Coulomb explosion is observed.

DOI: 10.1103/PhysRevLett.133.073202

The conversion of a significant fraction of laser energy into ion kinetic energy is a feature obtained in the interaction of intense laser light with dense matter [1]. In this context, atomic [2] and molecular clusters [3] offer unique opportunities to study basic mechanisms of light-matter interactions [4,5]. A variety of experimental results emphasize the generation of highly charged and energetic ions [6,7], fast electrons [8] and short wavelength radiation [9]. To decipher the dynamics, delayed plasmon-enhanced absorption plays a key role and this allows the main features to be understood [10]. With respect to ion emission, recoil energies exceeding 1 MeV have been obtained [7], whereas the maximum energy and the shape of the spectrum depends on the laser pulse envelope [11,12]. On a longer timescale, three-body recombination [13] has to be considered. Only recently it was demonstrated that the final products of the Coulomb explosion consist of a significant fraction of highly charged ions with electrons in high-lying Rydberg states [14].

An in-depth analysis of the ultrafast dynamics of cluster Coulomb explosions faces a number of challenges. In terms of ion diagnostics, the contribution of individual charge states z to the recoil energy spectrum is of considerable interest. But so far, resolving the underlying z distributions was given low attention [14–17]. Another problem, which has to be considered in high intensity laser studies is focal averaging [18], i.e., depending on the position within the focal volume, particles are exposed to different laser intensities, which has a significant impact on the particle energies [19]. Moving away from the focal point, the effective volume illuminated at a given intensity increases disproportionately. That leads to strong contributions from signals originating from the low-intensity regions to the overall yields. Therefore, it remains a challenge to obtain purified intensity-selective signals.

Strategies have been developed in order to solve the problem of focal averaging [20–22], which might blur detailed information encoded in the experimental signals. Intensity selective scanning [20] samples the focal region slice by slice. Corresponding experiments on clusters have been reported [23,24]. In practice, e.g., the width of the molecular beam is restricted by a narrow slit and the laser focus is shifted with respect to the particle beam. However, the displacement of the light focus places high demands on the laser beam quality. Moreover, in order to obtain a sufficiently resolved intensity-selective scanning profile, the position of the focus must be displaced in small steps. A more direct and less laborious approach is the intensity-difference spectrum technique (IDS) [21]. The method allows to determine a single intensity-resolved spectrum in only two measurements, i.e., ion spectra are recorded under slightly different intensity conditions and subtracted in the following.

In the present contribution, we extend our studies on argon cluster Coulomb explosions [25] by the combination of IDS with a charge-state selective ion energy spectrometry, which allows us to trace a hitherto undescribed transition from surface to volume expansion of ionized clusters.

The experimental setup to obtain charge-state resolved recoil energy spectra from the Coulomb explosion of clusters is described elsewhere [26]. Briefly, argon clusters Ar_N of mean size $\bar{N} = 3800$ are produced by supersonic

*Contact author: josef.tiggesbaeumker@uni-rostock.de

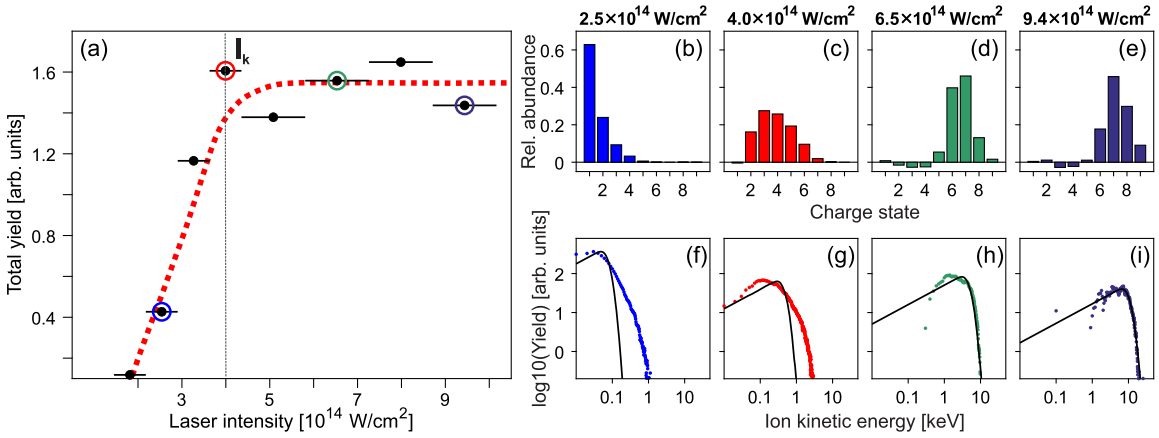

FIG. 1. (a) Intensity-resolved total ion yields Ar^{z+} from argon clusters ($\bar{N} = 3800$) obtained by applying the IDS method. The horizontal bars represent laser intensity ranges used to determine the intensity selective response. I_k marks the ionization of all cluster constituents. The red dotted line is used to guide the eye. (b)–(e) Examples of charge state distributions extracted by evaluating the experimental results. The negative values result from imperfections of the laser beam profile or laser power instabilities. (f)–(i) Corresponding IDS-analyzed total energy spectra of all ions obtained at the same laser intensities as (b)–(e). Solid lines represent fits based on the model of Islam *et al.* [33] and on parameters derived from the experiment such as cluster size and size distribution. At lower laser intensities (f), (g), the fits fail, which suggests a substantial change in the expansion dynamics.

expansion using a pulsed Even-Lavie source [27]. At a distance of 40 cm behind the nozzle, the particles are exposed to near-infrared ($\lambda_L = 793$ nm, $\tau_L = 180$ fs) laser pulses, having a Gaussian beam profile. The laser radiation is focused by a 30 cm lens to a spot diameter of 30 μm, giving intensities up to 10^{15} W/cm^2 at the focus. The laser power is controlled by an attenuator based on a $\lambda/2$ plate and a pair of Brewster type polarizers. Above the focus region the charge-state resolving ion energy analyzer is installed, see Ref. [26]. In a nutshell, energetic atomic ions from the Coulomb explosion are collimated by two slit apertures, pass a homogeneous magnetic field region, and finally hit a time- and position-sensitive delay line detector. Just before detection, the ions are accelerated by a potential difference of −2.3 keV. When determining the signal strengths, the different detection efficiencies are taken into account according to Ref. [28]. From the resulting time-of-flight–deflection histograms, charge-state selective recoil energy spectra are determined. The intensity-difference spectrum technique (IDS) (see Supplemental Material (Appendix A) [29]) using Gaussian laser beams is applied to obtain intensity-resolved signals. Measurements are conducted at different laser intensities $I_L = I_1, I_2, \ldots, I_n$, whereby $I_1 < I_2 < \ldots < I_n$. Using $[\log(I_m/I_{m-1})]^{-1}$ as a scaling factor, the differences of the signals $(Y_m - Y_{m-1})$ are calculated, i.e., the resulting spectra originate from the intensity ranges $[I_{m-1}: I_m]$. Note that instead of the laser intensity range, only the average value is mentioned in the following. The IDS method thus provides us with data under well-defined laser intensity conditions. We verified the applicability in experiments on barrier suppression ionization of atomic xenon (see Appendix B in Ref. [29]). Because of statistical fluctuations, especially at low count rates, negative IDS values sometimes occur [e.g., Fig. 1(i)]. Such rates cannot be represented in the chosen plot, which reduces the number of data points.

It is common practice (see, e.g., [34]), to record laser intensity dependencies of ion, electron, and x-ray emissions from cluster Coulomb explosions without decomposing the intensity distribution in the focus. A general observation is, that the yields increase with increasing laser intensity. Our measured total IDS ion yields Y_{total}, shown in Fig. 1(a), allow a more differentiated view. At an IDS center intensity $I = 1 \times 10^{14}$ W/cm^2, first emission of fast ions from Ar clusters can be detected in the experiment, indicating Coulomb explosion of the irradiated cluster. Above this threshold intensity, the ion signal strongly increases as function of I, in accordance with previous work [23]. The IDS analysis reveals that at higher intensities Y_{total} levels out, which suggests, that for $I \geq I_k = 4 \times 10^{14}$ W/cm^2 the overwhelming majority of cluster constituents are charged and that the particle explodes completely. Hence, the ever-increasing yields, as obtained in conventional focal averaging mode, is entirely due to the increase in focal volume (Appendix B in Ref. [29]).

The IDS charge state distributions (CSD) as well as the IDS energy spectra (ES) provide first information on the Coulomb explosion dynamics. Examples of CSDs are shown in Figs. 1(b)–1(e). At 2.5×10^{14} W/cm^2 the distribution spans from $z = 1$–5 with a maximum yield for Ar^{1+}. Emission of neutral atoms are also expected [17]. At I_k [Fig. 1(c)], the charge state increases up to $z = 7$ and the distribution maximizes at $z = 3$. Note, that singly charged ions are no longer observed. For $I > I_k$ a significant change in the CSD is obtained, see Figs. 1(d) and 1(e). Apart from peak shifts in the distributions towards higher z, distinct

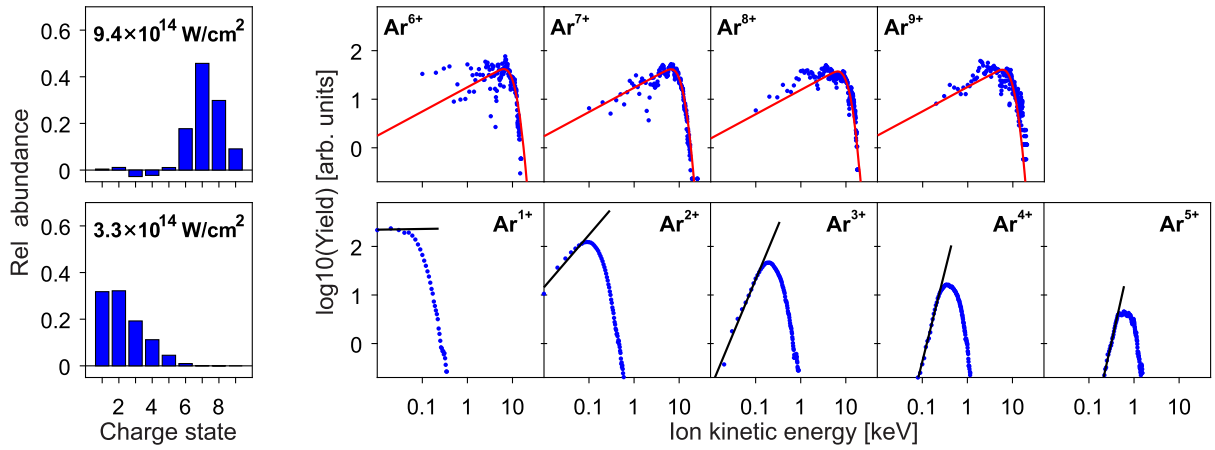

FIG. 2. Charge state distributions and corresponding charge-state resolved energy spectra recorded for selected IDS intensities: Top: The spectra for $I = 9.4 \times 10^{14}$ W/cm^2 correspond to ionization saturation conditions. Red lines represent fits based on the HCS model [33]. Bottom: The spectra for $I = 3.3 \times 10^{14}$ W/cm^2 reflect an ionization scenario below the onset of ionization saturation. The low-intensity energy spectra of the higher charge states show pronounced cutoffs at low recoil energies. The black solid lines serve to point out the increasing slope with z.

low-z cuts show up. Further, narrower CSDs stand out, which maximize near the highest z. The presence of a narrow peak at high z can be traced back to ionization saturation. In the nanoplasma, ionization takes place via electron impact. In this laser-driven process, however, the electrons must be accelerated to sufficiently high energies in order to be able to release more strongly bound core electrons. The significant increase in the ionization potentials of Ar (3ℓ: 144 eV; 2ℓ: 422 eV) [35] is the bottleneck, which reduces the generation of nanoplasma ion charge states significantly higher than $z_{\mathrm{sat}} = 8$. The maximum in the yields, however, is obtained at $z = 7$ instead of the expected $z = 8$, which gives a first hint that electron-ion recombination in the cluster disintegration plays a vital role [36]. The corresponding ES show clear changes in the envelopes, see Figs. 1(f)–1(i). Only the spectra (h), (i) at higher intensities, i.e., $I > I_{\mathrm{k}}$, are well reproduced by a model, which is based on the expansion of a homogeneously charged sphere (HCS) [33]. We note that a corresponding pattern is missing in similar experiments taken under focal averaging conditions, see the direct comparison in Appendix C of Ref. [29]. The IDS spectra thus hint at a marked change in the charging scenario near I_{k}. As a relevant feature and in view of the further discussion, we would like to point out that, in contrast to the CSD, the ES are sensitive to the time period in which the ions pick up an essential fraction of their recoil energies, i.e., under conditions of both short interatomic distances and high charge states. This characteristic is particularly pronounced upon rapid charging and reflects the temporal development of the ion charge states and the resulting Coulomb pressure.

The ion analyzer allows us to extract more detailed information by taking the energy spectra in a charge-state resolved manner (CRES), see Fig. 2 for selected examples. At $I = 9.4 \times 10^{14}$ W/cm^2 (top), the envelopes of the CRES of Ar^{6+} to Ar^{9+} are similar to each other and the recoil energy maxima E_{max} exceed 10 keV. The profiles agree well with those expected from HCS-explosion (red lines) [33]. At $I = 3.3 \times 10^{14}$ W/cm^2 (bottom), the signals of Ar^+ and Ar^{2+} show yields spanning down to zero kinetic energy. But in contrast, Ar^{3+} and in particular Ar^{4+} and Ar^{5+} have pronounced low-energy cutoffs. Evidence of such a feature was already obtained in focal-averaged experiments on Ar_N for $z \geq 6$ [25]. However, the declines at the low-energy wings of the CRES (Fig. 2) are better resolved due to the improved intensity resolution and the cutoffs can already be observed at lower charge states, i.e., $z \geq 3$.

The outstanding sensitivity of the delay line detector technology allows us to state that, for the lower laser intensity, low-energy ions are entirely absent at higher charge states. The energy spectra therefore deviate significantly from the prediction of the uniform explosion of a homogeneously charged sphere. Obviously, a different scenario, i.e., a charge- and radius-dependent acceleration process is conceivable. The observed low-energy cutoffs suggest that the corresponding highly charged ions originate from the surface region. Thus, the broad distributions of Ar^+ and Ar^{2+} in the low energy range result from ions, which reside within the core region of the cluster.

This evidence is supported by the following perspective on nanoplasma formation. It is generally accepted that in strong field cluster ionization, highly charged ions are generated in the entire particle. The developing deep mean field potential, however, traps a significant fraction of quasifree electrons [5], which effectively screen the charged ions. These delocalized electrons concentrate at the center of the nanoplasma [37] and slow down the expansion of the ions present there. Evidence for this core

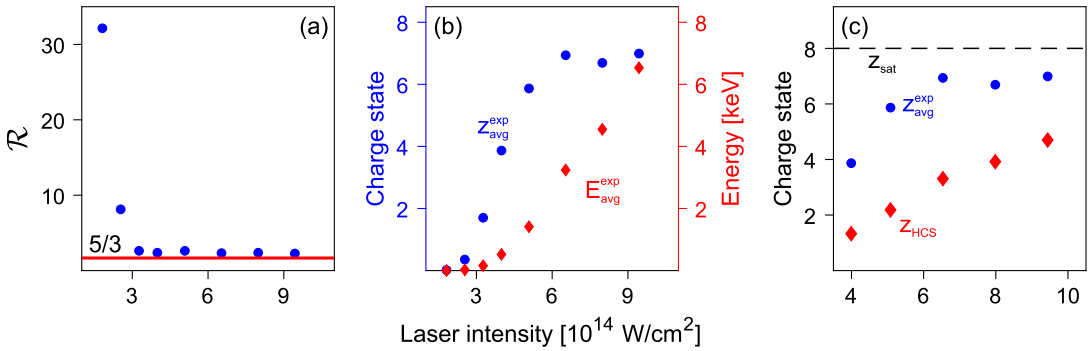

FIG. 3. Laser-intensity dependent development of (a) the ratio $\mathcal{R}$ of the experimental maximum $E_{\max}$ and average recoil energies $E_{\text{avg}}^{\text{exp}}$ (blue ○) compared to the theoretical value (red solid line), (b) experimental average charge state $z_{\text{avg}}^{\text{exp}}$ (blue ○) and recoil energy $E_{\text{avg}}^{\text{exp}}$ (red ◇), and (c) the average charge state ($z_{\text{avg}}^{\text{exp}}$, blue ○) compared to the model (Appendix D in Ref. [29]): (z_{HCS}, red ◇), z_{sat} (dashed line), ionization saturation limit.

screening is obtained in the substantial lower recoil energies, when the laser intensity is decreased below I_{k}. For example, reducing the laser intensity by a factor of 3 (Fig. 1) leads to a tenfold decrease in the maximum recoil energy $E_{\max}$. Beside screening, recombination may take place in the early phase of the explosion. Experimental studies and molecular dynamics simulations [38,39] point out a higher recombination rate at the core compared to the surface. As a consequence the effective charge state of the central region decreases and the expansion rate reduces. Other scenarios like high charge states are exclusively produced near the surface or high-z ions at the core pass low-z ions and gain additional energy can be ruled out.

The present nanoplasma conditions can be analyzed by considering the ratio between maximum and average energy, i.e., $\mathcal{R} = E_{\max}/E_{\text{avg}}$. For HCS expansion, a ratio of $\mathcal{R} = 5/3$ is determined [40]. The experimental $E_{\max}$ is defined as 10% of the maximum signal of the total ES [see Fig. 3(a)]. The comparison to the experimental $\mathcal{R}$ provides a measure to characterize the nonuniformity of the expansion. For $I > I_{\text{k}}$, values close to 5/3 are obtained. Analyzing the results at a lower I, the ratio increases significantly, e.g., $\mathcal{R} = 32$ for $I = 1.8 \times 10^{14}$ W/cm^2.

Summing up, the IDS measurements show a clear change in the structure of the spectra as a function of laser intensity (see Fig. 2). At intensities close to I_{k} a transition from "surface explosion, core expansion" to "homogeneous nanoplasma expansion" takes place, which confirms previous theoretical considerations [37].

The results suggest that apart from relaxation on the long timescale [14,41], ion screening by quasi-free electrons and three-body recombination plays an essential role also during the impact of the laser pulse. In the following, we evaluate the impact of ion screening and three-body recombination on the expansion. An in-depth view at surface-driven expansion requires molecular dynamics studies, which are beyond the scope of this work. The volume-driven Coulomb explosion obtained at higher laser intensities ($I > I_{\text{k}}$), however, can be classified on the basis of HCS (Appendix D [29]). The model gives us a relation between nanoplasma radius and charge state, as well as the resulting recoil energies. Based on the experimental mean charge states ($z_{\text{avg}}^{\text{exp}}$) and recoil energies ($E_{\text{avg}}^{\text{exp}}$) [Fig. 3(b)] as input, a comprehensive analysis within the framework of HCS shows that the charge states obtained in the measurements are higher than predicted. This encourages a more thorough view on the intensity dependence of the ion charge states. The description of the complex ionization and expansion dynamics simplifies, when taking advantage of the enhanced energy absorption from the laser field near the plasmon resonance [42], that is at the corresponding critical radius, where a sudden and substantial increase of the nanoplasma charge state can be achieved [5]. For $I \geq I_{\text{k}}$ such an efficient energy capture by resonant coupling is expected. That is because considering the experimental results, the expanding (HCS-)nanoplasma can attain the critical radius within the laser pulse. Taking this charging scenario into account, the HCS model can be used to derive a corresponding average charge state z_{HCS} (Appendix D [29], Eq. S9), see Fig. 3(c). In fact, due to resonance enhanced energy absorption, but limited by ionization saturation, $z_{\text{sat}} = 8$ is the resulting actual charge state for $I \geq I_{\text{k}}$. This leads to deep mean field potentials, which bind plasma electrons. Note that these quasi-free electrons are not included in HCS. Hence, a marked fraction of the electrons are confined by the mean field potential ($z_{\text{sat}} - z_{\text{HCS}}$), which might either recombine with the ions ($z_{\text{sat}} - z_{\text{avg}}^{\text{exp}}$) or are expelled later in the expansion ($z_{\text{avg}}^{\text{exp}} - z_{\text{HCS}}$).

Based on the IDS-results for $I \geq I_{\text{k}}$, the simplified HCS-analysis shows, that in addition to the substantial fraction of the electrons, which are confined by the mean-field potential, recombination is strongly suppressed. This is justified by the strong dependence of three-body recombination on plasma electron temperature ($\propto T_e^{-9/2}$) [43]. The ever enhanced energy absorption at higher laser intensities

increases T_e and thus increasingly suppresses recombination. As a result outer ionization is reinforced and the average charged state increases.

A significant contribution that is not taken into account so far is autoionization of Rydberg states [41]. During plasma expansion, quasi-free electrons recombine in high-lying Rydberg levels. The present ionization state leads to a corresponding recoil energy through the interaction with the plasma environment. Delayed Auger decay increases z and the ion is detected as having a higher charge. Further, the measured kinetic energies actually originate from an initially lower charge state. If such Auger decays take place before the ions enter the analyzer, a higher charge state is detected [14]. This results in a shift of the charge state distributions to larger values. The presence of a quasi-free electron cloud even at the highest laser intensities reveals that the core-region ions are still screened by plasma electrons. Although the energy spectra solely suggest a volume expansion for $I \geq I_k$ [Figs. 1(i) and 2 top], this treatment supports that the surface-to-volume transition is not yet complete even at maximum intensity.

The detailed analysis of the intensity-dependent transition from surface- to volume-driven Coulomb explosion points out a first view on the subtle interplay between charging and relaxation processes in the direct interaction of the nanoplasma with the laser field. In the future, the laser intensity difference technique, further improved preparation techniques like size-selected cluster targets, and high resolution spectrometry methods will offer prospects to capture previously inaccessible strong-field many-body dynamics. Thus, the course has been set towards atto-nano science studies [44,45] on free nanoparticles on a level previously only accessible in experiments on atoms and molecules.

Acknowledgments—We like to thank Thomas Fennel for helpful discussions on the subject. The Deutsche Forschungsgemeinschaft (TI 210/13-1, SFB 652, and SFB 1477 "Light-Matter Interactions at Interfaces," Project No. 441234705) is gratefully acknowledged for financial support.

D. K. and K. R. contributed equally to this work.

[1] E. Esarey, P. Sprangle, J. Krall, and A. Ting, Overview of plasma-based accelerator concepts, Trans. Plas. Sci. **24**, 252 (1996).

[2] A. McPherson, B. Thompson, A. Borisov, K. Boyer, and C. Rhodes, Multiphoton-induced x-ray emission at 4–5 keV from Xe atoms with multiple core vacancies, Nature (London) **370**, 631 (1994).

[3] S. G. Sayres, M. W. Ross, and A. W. Castleman, Influence of clustering and molecular orbital shapes on the ionization enhancement in ammonia, Phys. Chem. Chem. Phys. **13**, 12231 (2011).

[4] U. Saalmann, C. Siedschlag, and J. M. Rost, Mechanisms of cluster ionization in strong laser pulses, J. Phys. B **39**, R39 (2006).

[5] T. Fennel, K.-H. Meiwes-Broer, J. Tiggesbäumker, P.-G. Reinhard, P. M. Dinh, and E. Suraud, Laser-driven nonlinear cluster dynamics, Rev. Mod. Phys. **82**, 1793 (2010).

[6] E. M. Snyder, S. A. Buzza, and A. W. Castleman, Jr., Intense field-matter interactions: Multiple ionization of clusters, Phys. Rev. Lett. **77**, 3347 (1996).

[7] T. Ditmire, J. Tisch, E. Springate, M. Mason, N. Hay, R. Smith, I. Marangos, and M. Hutchinson, High-energy ions produced in explosions of superheated atomic clusters, Nature (London) **386**, 54 (1997).

[8] E. Springate, S. A. Aseyev, S. Zamith, and M. J. J. Vrakking, Electron kinetic energy measurements from laser irradiation of clusters, Phys. Rev. A **68**, 053201 (2003).

[9] R. Issac, G. Vieux, B. Ersfeld, E. Brunetti, S. Jamison, J. Gallacher, D. Clark, and D. Jaroszynski, Ultra hard x-rays from krypton clusters heated by intense laser fields, Phys. Plasmas **11**, 3491 (2004).

[10] T. Döppner, T. Fennel, T. Diederich, J. Tiggesbäumker, and K.-H. Meiwes-Broer, Controlling the Coulomb explosion of silver clusters by femtosecond dual-pulse laser excitation, Phys. Rev. Lett. **94**, 013401 (2005).

[11] Y. Fukuda, K. Yamakawa, Y. Akahane, M. Aoyama, N. Inoue, H. Ueda, and Y. Kishimoto, Optimized energetic particle emissions from Xe clusters in intense laser fields, Phys. Rev. A **67**, 061201(R) (2003).

[12] E. Skopalová, Y. C. El-Taha, M. H. A. Zaïr, E. Springate, J. W. G. Tisch, R. A. Smith, and J. P. Marangos, Pulse-length dependence of the anisotropy of laser-driven cluster explosions: Transition to the impulsive regime for pulses approaching the few-cycle limit, Phys. Rev. Lett. **104**, 203401 (2010).

[13] H. Bethe and E. Salpeter, *Quantum Mechanics of One- and Two-Electron Atoms* (Plenum Press, New York, 1977).

[14] D. Komar, L. Kazak, M. Almassarani, K.-H. Meiwes-Broer, and J. Tiggesbäumker, Highly charged Rydberg ions from the Coulomb explosion of clusters, Phys. Rev. Lett. **120**, 133207 (2018).

[15] M. Lezius, S. Dobosz, D. Normand, and M. Schmidt, Explosion dynamics of rare gas clusters in strong laser fields, Phys. Rev. Lett. **80**, 261 (1998).

[16] M. Hirokane, S. Shimizu, M. Hashida, S. Okada, S. Okihara, F. Sato, T. Iida, and S. Sakabe, Energy distributions of ions emitted from argon clusters Coulomb-exploded by intense femtosecond laser pulses, Phys. Rev. A **69**, 063201 (2004).

[17] R. Rajeev, T. M. Trivikram, K. Rishad, V. Narayanan, E. Krishnakumar, and M. Krishnamurthy, A compact laser-driven plasma accelerator for megaelectronvolt-energy neutral atoms, Nat. Phys. **9**, 185 (2013).

[18] R. Kopold, W. Becker, M. Kleber, and G. G. Paulus, Channel-closing effects in high-order above-threshold ionization and high-order harmonic generation, J. Phys. B **35**, 217 (2002).

[19] A. Heidenreich and J. Jortner, Kinetic energy distribution of multiply charged ions in Coulomb explosion of Xe clusters, J. Chem. Phys. **134**, 074315 (2011).

[20] M. A. Walker, P. Hansch, and L. D. Van Woerkom, Intensity-resolved multiphoton ionization: Circumventing spatial averaging, Phys. Rev. A **57**, R701(R) (1998).
[21] P. Wang, A. Sayler, K. Carnes, B. Esry, and I. Ben-Itzhak, Disentangling the volume effect through intensity-difference spectra: Application to laser-induced dissociation of H_2^+, Opt. Lett. **30**, 664 (2005).
[22] Y. Yao, W. M. Freund, J. Zhang, and W. Kong, Volume averaging effect in nonlinear processes of focused laser fields, J. Chem. Phys. **155**, 064202 (2021).
[23] T. Döppner, J. Müller, A. Przystawik, S. Göde, J. Tiggesbäumker, K.-H. Meiwes-Broer, C. Varin, L. Ramunno, T. Brabec, and T. Fennel, Steplike intensity threshold behavior of extreme ionization in laser-driven Xe clusters, Phys. Rev. Lett. **105**, 053401 (2010).
[24] S. G. Sayres, M. W. Ross, and A. W. Castleman, Onset of Coulomb explosion in small silicon clusters exposed to strong-field laser pulses, New J. Phys. **14**, 055014 (2012).
[25] D. Komar, L. Kazak, K.-H. Meiwes-Broer, and J. Tiggesbäumker, Development of ion recoil energy distributions in the Coulomb explosion of argon clusters resolved by charge-state selective ion energy spectroscopy, Eur. Phys. J. Spec. Top. **230**, 3989 (2021).
[26] D. Komar, K.-H. Meiwes-Broer, and J. Tiggesbäumker, High performance charge-state resolving ion energy analyzer optimized for intense laser studies on low-density cluster targets, Rev. Sci. Instrum. **87**, 103110 (2016).
[27] D. Pentlehner, R. Riechers, B. Dick, A. Slenczka, U. Even, N. Lavie, R. Brown, and K. Luria, Rapidly pulsed helium droplet source, Rev. Sci. Instrum. **80**, 043302 (2009).
[28] M. Krems, J. Zirbel, M. Thomason, and R. D. DuBois, Channel electron multiplier and channel plate efficiencies for detecting positive ions, Rev. Sci. Instrum. **76**, 093305 (2005).
[29] See Supplemental Material at http://link.aps.org/supplemental/10.1103/PhysRevLett.133.073202, which includes Refs. [30–32], for additional information about the IDS method and a detailed description of the analysis on the basis of HCS.
[30] J. Wiese, J.-F. Olivieri, A. Trabattoni, S. Trippel, and J. Küpper, Strong-field photoelectron momentum imaging of OCS at finely resolved incident intensities, New J. Phys. **21**, 083011 (2019).
[31] S. Augst, D. D. Meyerhofer, D. Strickland, and S. L. Chin, Laser ionization of noble gases by Coulomb-barrier suppression, J. Opt. Soc. Am. B **8**, 858 (1991).
[32] M. V. Ammosov, N. B. Delone, and V. P. Kraĭnov, Tunnel ionization of complex atoms and of atomic ions in an alternating electromagnetic field, Sov. Phys. JETP **64**, 1191 (1986).
[33] M. R. Islam, U. Saalmann, and J. M. Rost, Kinetic energy of ions after Coulomb explosion of clusters induced by an intense laser pulse, Phys. Rev. A **73**, 041201(R) (2006).
[34] M. Krishnamurthy, J. Jha, D. Mathur, C. Jungreuthmayer, L. Ramunno, J. Zanghellini, and T. Brabec, Ion charge state distribution in the laser-induced Coulomb explosion of argon clusters, J. Phys. B **39**, 625 (2006).
[35] W. M. Haynes, D. R. Lide, and T. J. Bruno, *CRC Handbook of Chemistry and Physics* (CRC Press, Boca Raton, FL, 2016).
[36] K. Ishikawa and T. Blenski, Explosion dynamics of rare-gas clusters in an intense laser field, Phys. Rev. A **62**, 063204 (2000).
[37] C. Jungreuthmayer, M. Geissler, J. Zanghellini, and T. Brabec, Microscopic analysis of large-cluster explosion in intense laser fields, Phys. Rev. Lett. **92**, 133401 (2004).
[38] L. Schroedter, M. Müller, A. Kickermann, A. Przystawik, S. Toleikis, M. Adolph, L. Flückiger, T. Gorkhover, L. Nösel, M. Krikunova, T. Oelze, Y. Ovcharenko, D. Rupp, M. Sauppe, D. Wolter, S. Schorb, C. Bostedt, T. Möller, and T. Laarmann, Hidden charge states in soft-x-ray laser-produced nanoplasmas revealed by fluorescence spectroscopy, Phys. Rev. Lett. **112**, 183401 (2014).
[39] D. Rupp, L. Flückiger, M. Adolph, T. Gorkhover, M. Krikunova, J. P. Müller, M. Müller, T. Oelze, Y. Ovcharenko, B. Röben, M. Sauppe, S. Schorb, D. Wolter, R. Mitzner, M. Wöstmann, S. Roling, M. Harmand, R. Treusch, M. Arbeiter, T. Fennel, C. Bostedt, and T. Möller, Recombination-enhanced surface expansion of clusters in intense soft x-ray laser pulses, Phys. Rev. Lett. **117**, 153401 (2016).
[40] I. Last and J. Jortner, Electron and nuclear dynamics of molecular clusters in ultraintense laser fields. III. Coulomb explosion of deuterium clusters, J. Chem. Phys. **121**, 3030 (2004).
[41] B. Schütte, M. Arbeiter, T. Fennel, G. Jabbari, A. Kuleff, M. J. J. Vrakking, and A. Rouzée, Observation of correlated electronic decay in expanding clusters triggered by near-infrared fields, Nat. Commun. **6**, 8596 (2015).
[42] L. Köller, M. Schumacher, J. Köhn, S. Teuber, J. Tiggesbäumker, and K.-H. Meiwes-Broer, Plasmon-enhanced multi-ionization of small metal clusters in strong femtosecond laser fields, Phys. Rev. Lett. **82**, 3783 (1999).
[43] Y. Hahn, Electron-ion recombination processes—an overview, Rep. Prog. Phys. **60**, 691 (1997).
[44] P. Hommelhoff and M. Kling, eds., *Attosecond Nanophysics—From Basic Science to Applications* (Wiley-VCH, Weinheim, 2015).
[45] M. F. Ciappina *et al.*, Attosecond physics at the nanoscale, Rep. Prog. Phys. **80**, 054401 (2017).